Experimental EOS determination of aluminum at Mbar pressure

CHEN Jianping[1,2], LI Ruxin[1], ZENG Zhinan[1], WANG Xingtao[1] & XU Zhizhan[1]

1. Shanghai Institute of Optics and Fine Mechanics, Shanghai 201800, China;
2. Beijing Aeronautical Technology Research Center, Beijing 100076, China
Correspondence should be addressed to Chen Jianping (email: chenjianping@mail.siom.ac.cn)
Received November 17, 2003

Abstract A shock wave is driven by a laser pulse of 1.2 ps duration (FWHM), with the intensity of ~10^{14} W/cm^2 at 785 nm, irradiating a 500 nm thick aluminum foil. A chirped laser pulse split from the main pulse is used to detect the shock breakout process at the rear surface of the target based on frequency domain interferometry. The mean shock velocity determination benefits from the precise synchronization (<100fs resolution) of the shock pump and probe laser pulses, which is calculated from the time the shock takes to travel the 500 nm thick aluminum. The released particle velocity determination benefits from the chirped pulse frequency domain interferometry. The average shock velocity is 15.15 km/s and the shock release particle velocity is 15.24 km/s, and the corresponding pressure after shock is 3.12 Mbar under our experimental condition.

Keywords: shock wave, equation of state, chirped laser pulse.

DOI: 10.1360/03yw0059

Equations of state (EOS) of matter at Mbar pressure are fundamental to numerous applications such as in astrophysics[1], plasma physics[2], inertial confinement fusion[3−6], and other related fields. Laser directly and indirectly induced shock wave compression of materials is an effective way to access these material states. Many recent experiments have been devoted to the study of laser driven shock waves and their use in the EOS measurement of strongly compressed materials[7].

It is well known that absolute EOS measurements require the simultaneous measurement of two shock parameters[8], such as shock wave velocity (D) and particle velocity (u) after shock. The first measurement of these two parameters has been performed in liquid deuterium by Collins et al.[9] with a large dimension laser system like Nova. The shock and particle velocities are deduced from the shock front and interface slope in the transverse streak transmission radiograph of a D_2 EOS target with a Be pusher at a laser intensity of 7.6×10^{13} W/cm^2. Another simultaneous measurements of shock and particle velocity in silica with a small dimension laser was performed by Benuzzi-Mounaix et

al.[10], who used chirped pulse frequency-domain interferometry (FDI).

The natural approach to determining shock wave velocity in an opaque media is to image the optical flash when the shock wave breaks out of a step-like foil target with a streak camera (at a resolution of several picoseconds)[7,11]. The streak image shows the shock breakout at two times corresponding to the two-step thickness; the time interval between the breakouts measures the shock speed in the target, with the shock speed being assumed constant. The problems associated with interpreting optical flashes that accompany the emergence of strong shock wave at the free surface of an opaque metal are well known[8]. At the resolution of several picoseconds, the recorded optical flashes by the streak camera are from an emitting layer with optical length of about 1 to the vacuum boundary[8].

The common method for determining particle velocity is the velocity interferometer system for any reflector (VISAR) design of Barker and Hollenbach[12]. But the time resolution (>75 ps) is low. Recent work by Evans et al.[13] and Gahagan et al.[14] showed the possibility of measuring the fluid velocity of shocked aluminum by using the frequency interferometer, and deduced shock velocity by measuring the shock breakout time with targets of different thickness by assuming that shot to shot energy fluctuations were negligible. After that, constant efforts are currently devoted to improving their signal-to-noise level and accuracy.

In this paper, we show the feasibility of simultaneous measurement of shock velocity and released particle velocity after shock at Mbar pressure with pump-probe and chirped pulse spectral interferometry technique at one laser pulse. Similar purpose has been achieved by Benuzzi-Monuaix et al. with a VISAR diagnostic and step targets[10]. In our experiment, the shock wave is driven by a laser pulse of 1.2 ps duration (FWHM), with the intensity of ~10^{14} W/cm^2 at 785 nm, irradiating a 500 nm thick aluminum foil. A chirped laser pulse split from the main pulse is used to detect the shock release process at the rear surface of the target based on spectral interferometry. The time interval between the shock pump and probe pulses is determined precisely at less than 100 fs resolution, so the mean shock velocity can be calculated from the time the shock takes to travel the 500 nm thick aluminum. The released particle velocity determination benefits from the chirped pulse frequency interferometry. The experimental data meet the previous empirical formula for shock and particle velocities and this indicates that the two measured parameters are self-consistent.

1 Experimental method

The experiments are performed with a 10-Hz chirped-pulse amplification Ti: sapphire laser system, which can deliver laser pulses with a duration of 34 fs and the output energy as great as 1 J. A linearly positive chirped pulse of 1.2 ps (FWHM) is deliberately generated from the laser system by slightly shortening the distance between the two gratings of the pulse compressor.

The targets used in these experiments are the aluminum layer of 500 nm thickness coated onto the 1 μm thick polythene film substrate. The root mean square roughness of the aluminum surface is less than 10 nm measured with an AFM. This thickness of aluminum is chosen to ensure that the aluminum rear surface will not be perturbed by the decaying heat conduction wave during the observation time interval and for the laser irradiances that we have used[13,15]. The polythene film is transparent for the 1.2 ps laser pulse with the intensity of ~10^{14} W/cm^2 at 785 nm wavelength and this has been checked in the experiments. The target is mounted on a translation stage.

The experimental arrangement is shown in Fig. 1. Details of the experimental approach can also be found in ref. [16]. The synchronization of the pump and the probe pulses is performed in two steps. First, we synchronize the pump and the probe pulses. Second, we perform the synchronization of the probe and the reference pulses.

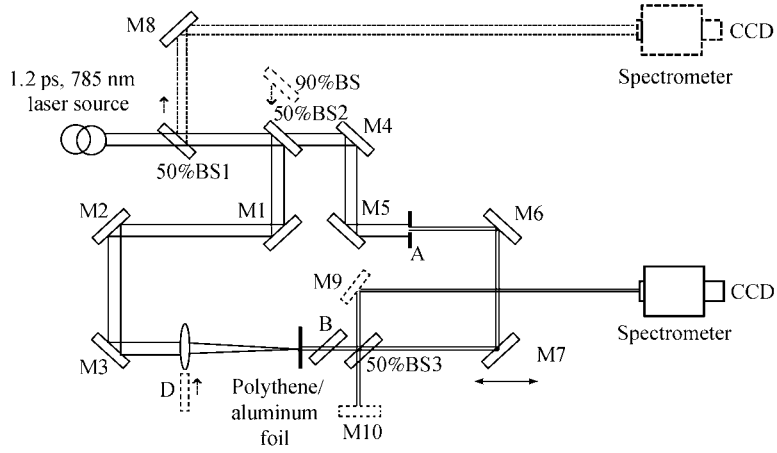

Fig. 1. Schematic diagram of the experimental setup. M1-M9, reflector at 45° for 785 nm; M10, reflector at 0° for 785nm; BS, beam splitter; A, 2 mm aperture; B, compensation plate for 50%BS3; C, compensation plate for the convex lens D. M6 and M7 are mounted on a timing slide. The diagram in solid lines is for shock pump and probe synchronization purpose. While for shock and released particle velocity experimental operation, C and 50%BS2 are replaced by D and 90%BS, respectively. 50%BS1 is moved away. M9 and M10 play their roles at this stage (see dash line).

After passing through 50%BS1, the pulse from the laser system is divided into two parts by 50%BS2. The reflected part of the laser pulse, served as the pump pulse, after relayed by M2 and M3, irradiates normally on the polythene/aluminum interface after passing through the compensation plate C for a convex lens D. The transmitted part from 50%BS2 is relayed by M4-M7, and also irradiates normally on the rear surface of the aluminum foil after passing through 50%BS3 and a compensation plate B. The two pulses irradiating normally on the aluminum foil in opposite directions are concentric with each other.

The pump and the probe pulses reflected by the front and rear surface of aluminum, respectively, are recollected and collimated by 50%BS1, and sent into the spectrometer by M8. The two pulses interfere[17—20] in the spectrometer and the interferograms are

visualized at the output of the spectrometer on a CCD camera interfaced with a microcomputer. Adjust the translation slide mounted with M6 and M7 until the fringe spacing covers the size of the CCD detector. The synchronization precision of the pump and the probe pulses is less than 100 fs involving the angle error of the two pulses.

It is the basic condition for precisely synchronizing the pump and the probe pulses in this experiment that both the pump and the probe pulses irradiate normally on the aluminum surfaces in opposite directions and concentrically. In most previous experiments based on FDI technique, the probe pulse irradiated on the target at an oblique angle, so it is difficult for them to synchronize precisely the pump and probe pulses.

After the synchronizing operation of the pump and the probe pulses, 50%BS1 is moved away, and 50%BS2 is replaced by a 90%BS which reflects 90% of the laser pulse for shock pump purpose which is blocked at this stage. The weaker part of the laser pulse, passing through a 2 mm aperture (A in fig. 1) with the energy of ~ 4 μJ, is further divided by 50%BS3 into two parts which are fed, respectively, into the two arms (M10 and aluminum foil) of a Michelson interferometer as the reference and the probe pulses. The pulses reflected by the aluminum foil and M10 are sent into the spectrometer by M9, and they are displaced temporally by τ that can be changed by adjusting the reference arm (M10). The area of the target under study is imaged onto the slit (10 μm) at the entrance of the spectrometer. The spatial resolution along the slit is ~ 15 μm (one pixel of the CCD).

2 Experimental results

For shock pumping-and-probing operation, the compensation plate is replaced with a *f*/3 lens D which partially focuses the pump pulse normally onto the polythene/aluminum interface to generate a strong shock wave in the aluminum foil. At the focus, the laser intensity distribution is nearly Gaussian with 90% of the incident laser energy contained in a spot of 800 μm in diameter and 60% in a spot of 400 μm in diameter. The laser irradiance at the central 400 μm spot is ~10^{14} W/cm^2.

The probe pulse irradiates the rear side of the aluminum foil at normal incidence, and covers the pump spot concentrically. The aluminum foil is set as the probe arm of the Michelson interferometer. The reference pulse does not interact with the target foil, so that we can make absolute measurement of shock-induced phase shifts. M6 and M7 are mounted on a timing slide with a spatial resolution of 10 μm, corresponding to a temporal resolution of 67 fs. The pump-probe delay can be adjusted to 500 ps, while keeping the probe and the reference pulse separation constant. We move the target between two laser shots so that each laser shot irradiates a fresh part of the target. All measurements are conducted on a single-shot basis achieved by inserting a shutter into the laser source.

We have measured the quite early stage of shock breakout driven by 1.04×10^{14} W/cm^2 (at the central 400 μm spot) laser irradiance. The interferograms are recorded at

every 5 ps time interval from 3 to 33 ps with respect to the pump pulse. A corresponding reference interferogram is recorded before each pump of the shock. Fig. 2 shows the typical interferogram pictures before 33 ps (a) and at 33 ps (b). The horizontal axis of the two-dimensional image represents the wavelength, while the vertical axis (parallel to the slit) represents the radial (vertical) dimension. At horizontal axis, long wavelength is on the right hand and short wavelength is on the left, and the corresponding time axis is from right to left, as the probe pulse frequency is positively chirped. The vertical dimension of each graph is 4 mm. So the shock deformation process may be spatially resolved along the slit.

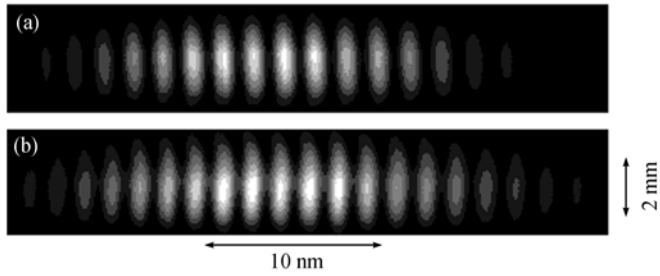

Fig. 2. Typical interferogram pictures before 33 ps (a) and at 33 ps (b). Shock-driven irradiance is 1.04×10^{14} W/cm^2 at the central 400 μm area. At horizontal axis, long wavelength is on the right hand and short wavelength is on the left, the corresponding time axis is from right to left, as the probe pulse frequency is positively chirped. The vertical dimension of each graph is 4 mm.

The experimental results indicate that before 33 ps, the interferograms involving pump lasers keep their shape as the corresponding reference ones. While at 33 ps, there are evident bends in the pumping interferograms, which indicates the arrival and break-out of the shock at the rear surface of the aluminum foil. In this paper, we only discuss the initial arrival of the shock; detailed phenomena discussion after shock release can be found in ref. [16].

3 Discussions

3.1 Signal reconstruction

A linearly chirped laser pulse can be written as $\omega(t)=\omega_0+at$, where ω_0 is the central frequency of the laser and a is the chirp rate which may be measured as[20]:

$$a=\frac{4\ln 2}{\Delta T_0\sqrt{\Delta T^2-\Delta T_0^2}},$$

where ΔT_0 is the Fourier-limited duration of the laser pulse. The field of the chirped pulse can be written in the frequency domain

$$E_0(\omega)=\varepsilon_0(\omega)\exp(i(\omega-\omega_0)^2/a).$$

Before the shock arrives at the rear surface of the target, the resulting interference signal

of the reference and probe pulses at the output of the spectrometer is represented by the following proportion:

$$I(\omega) = \left|\varepsilon_0(\omega)\right|^2 (2 + 2\cos(\omega\tau)).$$

When the probe pulse interacts with the shock wave, the perturbed interference signal is[17]

$$I'(\omega) = \left|\varepsilon_0(\omega)\right|^2 (1 + R(\omega)^2 + 2R(\omega)\cos(\omega\tau + \Delta\phi)).$$

The inverse Fourier transform of $I(\omega)$ and $I'(\omega)$ shows two peaks in the time domain; the oscillating peaks are located at τ (see fig. 3). Isolating the lateral peaks and performing the Fourier transform back into frequency domain, we get I_{ref} and I_{signal}[17−19]:

$$I_{ref}(\omega) = \left|\varepsilon_0(\omega)\right|^2 e^{i\omega\tau},$$

$$I_{signal}(\omega) = \left|\varepsilon_0(\omega)\right|^2 R(\omega) e^{i(\omega\tau + \Delta\phi(\omega))}.$$

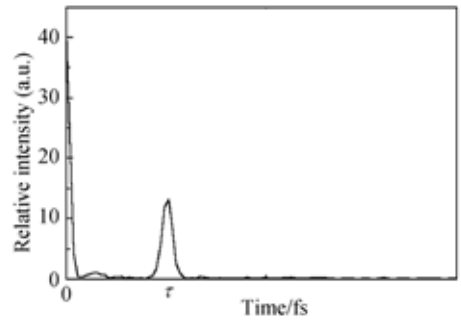

Fig. 3. Inverse Fourier transform of the interferograms.

The complex perturbation in the frequency-domain is

$$P(\omega) = \frac{I_{signal}(\omega)}{I_{ref}(\omega)} = R(\omega) e^{i\Delta\phi(\omega)},$$

where $R(\omega)$ is reflection coefficient and $\Delta\phi(\omega)$ is the phase shift difference between the perturbed and unperturbed target surface. The shock perturbed phase shift at time domain can now be recovered as[20]

$$P(t) = F^{-1}(E_0(\omega)P(\omega)) / E_0(t).$$

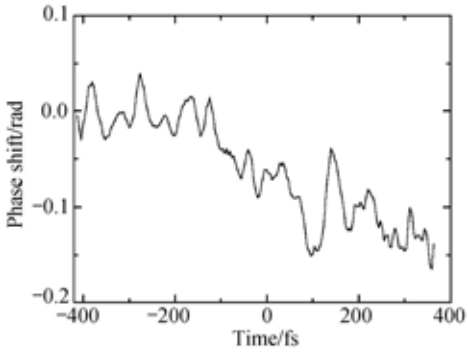

Fig. 4. A phase shift signal reconstructed from the center lineout in fig. 2(b).

Fig. 4 shows the phase shift signal reconstructed from the center lineout in fig. 2. The high frequency fluctuations in the phase shift line arise from one pixel resolution of the CCD camera and finite roughness of the foil surface (<10 nm). The time zero corresponds to 785 nm of the chirped probe pulse.

3.2 EOS determination

At 33 ps probe delay time, the evident interferogram bends in fig. 2(b) are also shown as the phase decrease in fig. 4 which be-

gins at ~–100 fs. This indicates an accurate arrival time (32.9±0.1 ps after the pumping pulse) of the shock at the rear surface of the foil. Correspondingly, the mean shock velocity at which it travels the 500±10 nm aluminum foil can be calculated as 15.15±0.3 km/s for 1.04×10^{14} W/cm^2 pump laser irradiance.

There are three possible reasons for the observed phase shift[13], i.e. the motion of the aluminum foil surface, the changes in the optical properties of the aluminum foil surface, and the changes in the refractive index of the air near the foil. At the early time of shock deformation, the aluminum plasma scale length at the foil surface is much shorter than the laser wavelength, so that the last two contributions are negligible at the normal probe angle. The shock deforming velocity can be derived from the Doppler phase shift rate[13] as ~15.24 km/s. The corresponding particle velocity after shock in the foil could be half of the free unloading velocity[8] and it is determined to be ~7.62 km/s.

Now, two shock parameters have been measured simultaneously at one laser pulse, so the absolute EOS of the aluminum can be determined. For example, the shock pressure can be calculated[8] as $P = Du/V_0 = 3.12$ Mbar under our experimental condition, where $D = 15.15$ km/s and $u = 7.62$ km/s are shock and particle velocity, respectively, and $V_0 = 1/\rho_0$ with ρ_0 the unshocked aluminum density which is 2.6984 g/cm^3 in this case. This pressure value is comparable with that measured by Evans et al.[13] In their experiment, pressures 1—3 Mbar were measured along the aluminum Hugoniot curve for ~10^{14} W/cm^2, 120 fs laser irradiance and duration. The reason why we obtained a little higher intense shock pressure is because a longer duration laser (1.2 ps) is used in our experiment.

The shock velocity can also be deduced from the empirical equation for aluminum[21] $D = 5.471+1.310u = 15.45$ km/s, $u = 7.62$ km/s is the measured particle velocity. The difference between the calculated shock velocity value and the measured one comes from the following reasons. First, the chemical composition of the two targets is different and thus the two target materials have different EOSs, correspondingly. Second, the finite roughness of the aluminum target foil (<10 nm root mean square) contributes a lot to the shock velocity error. For example, the shock propagating through 500 nm of aluminum at 15.15 km/s will reach the back surface in 32.9 ps. A variation as small as 2% in thickness will cause 0.3 km/s error in the shock velocity. Last, the fluctuations arise from one pixel resolution of the CCD camera. The measured shock velocity and particle velocity are consistent if the forenamed error aspects have been taken into consideration. The estimated precision on particle velocity is ≤5%.

4 Conclusions

We have shown the feasibility of simultaneous measurement of shock velocity and released particle velocity after shock. Correspondingly, the EOS in aluminum after shock is determined experimentally. The shock velocity determination benefits from the precise synchronization (<100 fs resolution) of shock pump and probe laser pulses,

which is calculated from the time the shock takes to travel the 500 nm thick aluminum. The released particle velocity determination takes advantage of the chirped pulse frequency domain interferometry. The two measured parameters are self-consistent. Further work will be devoted to the simultaneous measurement of shock wave and particle velocities.

Acknowledgements We gratefully acknowledge the support of Prof. Lin Lihuang and Mr. Lu Haihe for the use of laser system where the experiments were carried out. We thank Dr. Wang Cheng, Yang Xiaodong, and Prof. Yu Wei and Han Shensheng for their helpful discussions. We also thank Gao Quanlan and Xiang Huizhu for the preparation of the aluminum foil.

References

1. Remington, B. A., Arnett, D., Drake, R. P., Modeling astrophysical phenomena in the laboratory with intense lasers, Science, 1999, 284: 1488—1493. [DOI]
2. Widmann, K., Guethlein, G., Foord, M. E. et al., Interfeometric investigation of femtosecond laser-heated expanded states, Phys. Plasmas, 2001, 8(9): 3869—3872. [DOI]
3. Cauble, R., Perry, T. S., Bach, D. R. et al., Absolute equation-of-state data in 10—40 Mbar (1—4 TPa) regime, Phys. Rev. Lett., 1998, 80(6): 1248—1251. [DOI]
4. Celliers, P. M., Collins, G. W., Da Silva, L. B. et al., Shock-induced transformation of liquid deuterium into a metal fluid, Phys. Rev. Lett., 2000, 84(24): 5564—5567. [DOI]
5. Santala, M. I. K., Zepf, M., Watts, I. et al., Effect of the plasma density scale length on the direction of fast electrons in relative laser-solid interactions, Phys. Rev. Lett., 2000, 84(7): 1459—1462. [DOI]
6. Sheng, Z. M., Sentoku, Y., Mima, K. et al., Angular distribution of fast electrons, ions, and bremsstrahlung x/γ-rays in intense laser interaction with solid targets, Phys. Rev. Lett., 2000, 85(25): 5340—5343. [DOI]
7. Cauble, R., Phillion, D. W., Hoover, T. J. et al., Demonstration of 0.75 Gbar planar shocks in X-ray driven colliding foils, Phys. Rev. Lett., 1993, 70(14): 2102—2105. [DOI]
8. Zel'dovich, Ya. B., Raizer, Yu. P., Physics of Shock Waves and High Temperature Hydrodynamic Phenomena, New York: Academic, 1966.
9. Collins, G. W., Da Silva, L. B., Celliers, P. et al., Measurement of the equation of state of deuterium at the fluid insulator-metal transition, Science, 1998, 281: 1178—1181. [DOI]
10. Benuzzi-Mounaix, A., Koenig, M., Boudenne, J. M. et al., Chirped pulse reflectivity and frequency domain interferometry in laser driven shock experiments, Phys. Rev. E, 1999, 60(3): R2488—R2491. [DOI]
11. Ng, A., Parfeniuk, D., DaSilva, L., Hugoniot measurement for laser-generated shock waves in aluminum, Phys. Rev. Lett., 1985, 54(24): 2604—2607. [DOI]
12. Barker, L. M., Hollenbach, R. E., Laser interferometer for measuring high velocities of any reflecting surface, J. Appl. Phys., 1972, 43(11): 4669—4675.
13. Evans, R., Badger, A. D., Falliès, F. et al., Time-and space-resolved optical probing of femtosecond-laser-driven shock waves in aluminum, Phys. Rev. Lett., 1996, 77: 3359—3362. [DOI]
14. Gahangan, K. T., Moore, D. S., Funk, D. J. et al., Measurement of shock wave rise time in metal thin film, Phys. Rev. Lett., 2000, 85(15): 3205—3208. [DOI]
15. Ng, A., Forsman, A., Celliers, P., Heat front propagation in femtosecond-laser-heated solids, Phys. Rev. E, 1995, 51(6): R5208—R5211. [DOI]
16. Chen, J. P., Li, R. X., Zeng, Z. N. et al., Shock-accelerated flying foil diagnostic with a chirped pulse spectral interferometry, Chin. Phys. Lett., 2003, 20(4): 541—543. [DOI]
17. Tokunaga, E., Terasaki, A., Kobayashi, T., Frequency-domain interferometry for femtosecond time-resolved phase spectroscory, Opt. Lett., 1992, 17(16): 1131—1133.
18. Scherer, N. F., Carlson, R. J., Matro, A. et al., Fluorescence-detected wave packet interferometry: time resolved molecular spectroscopy with sequences of femtosecond phase-locked pulses, J. Chem. Phys., 1991, 95(3): 1487—1511. [DOI]
19. Chien, C. Y., La Fontaine, B., Desparois, A. et al., Single-shot chirped-pulse spectral interferometry used to measure the femtosecond ionization dynamic of air, Opt. Lett., 2000, 25(8): 578—580.
20. Geindre, J. P., Audebert, P., Rebibo, S. et al., Singe-shot spectral interferometry with chirped pulses, Optics Lett., 2001, 26(20): 1612—1614.
21. Isbell, W. M., Shipman, F. H., Jones, A. H., Hugoniot Equation of State Measurements for Eleven Materials to Five Megabars, AD721920: 42.